

Relation Between Coating Parameters and Structural and Mechanical Properties of Magnetron Sputtered TiAlN Coatings

Şengül Danişman · Soner Savaş

Received: 22 February 2013 / Accepted: 31 May 2013 / Published online: 6 April 2014
© King Fahd University of Petroleum and Minerals 2014

Abstract In this paper, it is aimed to investigate the structural and mechanical properties of TiAlN coatings deposited by the magnetron sputtering method on silicon substrates using a compound $Ti_{0.5}Al_{0.5}$ target at different nitrogen partial pressures of 0.3, 0.6 and 1.2 mtorr, substrate bias voltages of 0, -100 and -200 V and target to substrate distances of 6, 11, 16 and 21 cm. Scanning electron microscopy, energy-dispersive X-ray spectroscopy, X-ray diffraction, atomic force microscopy, the CSEM nano-hardness tester and CSEM-Calotest were used to characterize the coatings. The results showed that the hardness and mechanical properties of the coatings increased at low nitrogen pressures and high bias voltages, and that target to substrate distance showed a significant effect on the structural and mechanical properties of the coatings. With a shorter target to substrate distance, densified TiAlN coatings of substantially higher hardness and Ti content were produced with enhanced deposition rate. Furthermore, 11 cm target to substrate distance was found as the critical distance for the hardness and Al content of the coatings, especially at low bias voltage and low nitrogen pressure, respectively. In addition, X-ray diffraction analysis in this study showed that short target to substrate dis-

tances and high bias voltages indicated significant effect on a (2 0 0) preferred orientation of the NaCl structure.

Keywords Titanium aluminium nitride · Magnetron sputtering · Target to substrate distance · Nano-hardness

الخلاصة

كان الهدف من هذه الورقة العلمية هو التحقيق في الخواص البنائية والميكانيكية لطلاءات TiAlN المرسبة باستخدام طريقة بصق المغنطرون فوق ملققات السيليكون باستخدام مركب $Ti_{0.5}Al_{0.5}$ المستهدف عند ضغوط نيتروجين جزئية مختلفة من 0.3 ، 0.6 ، 1.2 ميلي تور، وجهود ميل ملقم من 0، -100 و-200 فولت مسافات من الهدف إلى الملقم من 6، 11، 16 و 21 سم. وتم لتحقيق ذلك استخدام المجهر الإلكتروني الماسح، ومطيافية تشتت طاقة الأشعة السينية، وحيود الأشعة السينية، ومجهر القوة الذرية، وفاحص صلادة CSEM النانوي واختبار CSEM-Calotest في توصيف الطلاءات. وأظهرت النتائج أن الخواص الميكانيكية وصلادة هذه الطلاءات تزداد عند ضغوط نيتروجين منخفضة وجهود ميل مرتفعة، وأظهرت المسافة من الهدف إلى الملقم تأثيرا مهما في الخواص الميكانيكية والبنائية للطلاءات. ومع مسافة من الهدف إلى الملقم أقصر تم إنتاج طلاءات TiAlN كثيفة ذات صلادة مرتفعة بشكل كبير ومحتوى تيتانيوم مع معدل ترسيب معزز. أكثر من ذلك، فإن مسافة هدف إل ملقم من 11 سم وجدت أنها هي المسافة الحرجة لصلادة ومحتوى الألمنيوم للطلاءات، وبخاصة عند جهد ميل منخفض وضغط نيتروجين منخفض على التوالي. بالإضافة إلى ذلك، فقد أظهر تحليل حيود الأشعة السينية في هذه الدراسة أن المسافات القصيرة من الهدف إلى الملقم وجهود ميل مرتفعة تشير إلى تأثير مهم في موقع (2 0 0) المفضل لبنية كلوريد الصوديوم.

Ş. Danişman (✉)
Department of Mechanical Engineering, Faculty of Engineering,
Erciyes University, 38039 Talas, Kayseri, Turkey
e-mail: sdanisman@erciyes.edu.tr

S. Savaş
Department of Materials Science and Engineering, Faculty
of Engineering, Erciyes University, 38039 Talas, Kayseri, Turkey
e-mail: ssavas@erciyes.edu.tr

Ş. Danişman · S. Savaş
Surface Technologies Research and Application Laboratory, Faculty
of Engineering, Erciyes University, 38039 Talas, Kayseri, Turkey

1 Introduction

Ceramic coatings on various materials have shown significant improvements since 1970. Some of the well-known coating techniques are physical vapour deposition (PVD), chemical vapour deposition (CVD), sol-gel (SG), plasma spray (PS),

etc [1]. The first of these, in PVD coating, basic deposition processes are evaporation, sputtering and ion plating. The basic sputtering process has been known for many years and many materials have been successfully deposited using this technique. However, the process is limited by low deposition rates, low ionisation efficiencies in the plasma, and high substrate heating effects. These limitations have been overcome by the development of magnetron sputtering and, more recently, unbalanced magnetron sputtering. Consequently, magnetron sputtering, especially the unbalanced magnetron sputtering systems, now makes a significant impact in application areas including hard, wear-resistant coatings, low friction coatings, corrosion-resistant coatings, decorative coatings and coatings with specific optical, or electrical properties. Therefore, magnetron sputtering have been widely used for the deposition of thin films in industrial applications [2,3].

The bond structure in transition metal nitrides consists of a mixture of covalent, metallic and ionic components, and is responsible for high hardness, excellent wear resistance, chemical inertness, good electrical conductivity and superconducting properties. The interest in thin films of metal nitrides is growing rapidly for wear and corrosion resistant applications [4–7]. Especially, Ti-based hard ceramic films deposited by physical vapour deposition (PVD) techniques, such as titanium nitride (TiN), have been extensively studied and successfully used in different areas because of their desirable properties of high melting point, high hardness and wear resistance and high thermal conductivity [4,8,9]. By incorporation of aluminium in TiN film forms titanium aluminium nitride (TiAlN), which improves the oxidation behaviour and thermal stability of the coating [4,5,10]. The most important properties of TiAlN coatings are high hardness (~28–32 GPa), relatively low residual stress (~5 GPa), superior oxidation resistance, high hot hardness and low thermal conductivity. These features make TiAlN coatings most desirable in dry machining, the machining of abrasive alloys at high speeds, hot extrusion, die casting and cold drawing [4,11–17]. Furthermore, the formation of a protective, adhesive Al_2O_3 top layer at high temperatures increases the diffusion and oxidation resistance of TiAlN films by preventing oxygen diffusion to the coating [9,11,18–23].

Non-reactive as well as reactive versions of magnetron sputtering are based on the emission of film-forming surface atoms from the target by the impact of hyperthermal gas ions extracted from the plasma of a gas discharge [24]. The properties and performance of TiAlN coatings deposited by PVD techniques are largely affected by deposition parameters such as nitrogen pressure and bias voltage. Jeong et al. [25] found that the columns of TiAlN coatings became denser and finer grained morphology as the nitrogen flow rate increased. Ramana et al. [26] and Oliveira et al. [27,28] reported that the hardness of TiAlN coatings increased as the nitrogen content of the coating increased. Wuhner et al. [29]

showed that the deposition rate and hardness of the coatings decreased and their surface roughness increased when the nitrogen pressure increased. In addition, bias voltage has a significant effect on coating properties. Barshilia et al. [30] and Ramana et al. [26] found the optimum bias voltages as -75 and -100 V, respectively. However, Ahlgren et al. [31] reported that compressive residual stress also increased with increased bias voltage. The application of additional bias voltage is also probably necessary to achieve a superlattice structure with relatively smooth interfaces and, simultaneously, a dense nanocrystalline microstructure [32].

Although target to substrate distance (TSD) is a very important parameter in Ti-based coating properties, there is only a limited number of studies on the subject in the literature [29,33,34]. Wuhner et al. [29] showed that the coatings deposited with a 65 mm TSD were generally of higher hardness than coatings with a 110 mm TSD. Chen et al. [34] found that the deposition rate decreased and the Al/Ti ratio increased when the TSD increased from 57 to 85 mm. You et al. [33] also showed that the deposition rate decreased when the TSD increased from 30 to 100 mm. Panich et al. [35] found that the hardness and coating-substrate adhesion of the coatings deposited on stationary substrates were much higher than those deposited on rotating substrates.

This paper reports and discusses the inter-relationship between the nearer TSD, coating parameters and TiAlN coating properties in detail. The structural and mechanical properties of TiAlN coatings deposited by the magnetron sputtering method on Si(100) substrates using a compound $\text{Ti}_{0.5}\text{Al}_{0.5}$ target at different nitrogen partial pressures of 0.3, 0.6 and 1.2 mtorr, substrate bias voltages of 0, -100 and -200 V and target to substrate distances of 6, 11, 16 and 21 cm were investigated and the comparative properties were discussed.

2 Experimental Details

2.1 Coating Deposition

TiAlN coatings were deposited by the dual magnetron sputtering system shown in Fig. 1a on Si(100) substrates using a compound $\text{Ti}_{0.5}\text{Al}_{0.5}$ target (at. 50 % Ti-50 % Al). The system has a stainless steel vacuum chamber (600 mm in diameter and 800 mm high) and two unbalanced planar magnetrons powered by two independent 12 kW DC generators (12 MDX advanced energy). The system used also has a plasma emission monitoring (PEM) system for monitoring and controlling the reactive sputtering processes for the production of high-quality films, reproducibly. The sputtered species originated from a compound $\text{Ti}_{0.5}\text{Al}_{0.5}$ target with a size of about $645 \times 110 \times 10$ mm. The reactive sputtering process is very non-linear and usually exhibits a hysteresis behaviour with respect to the reactive gas flow [36,37]. To optimize the coat-

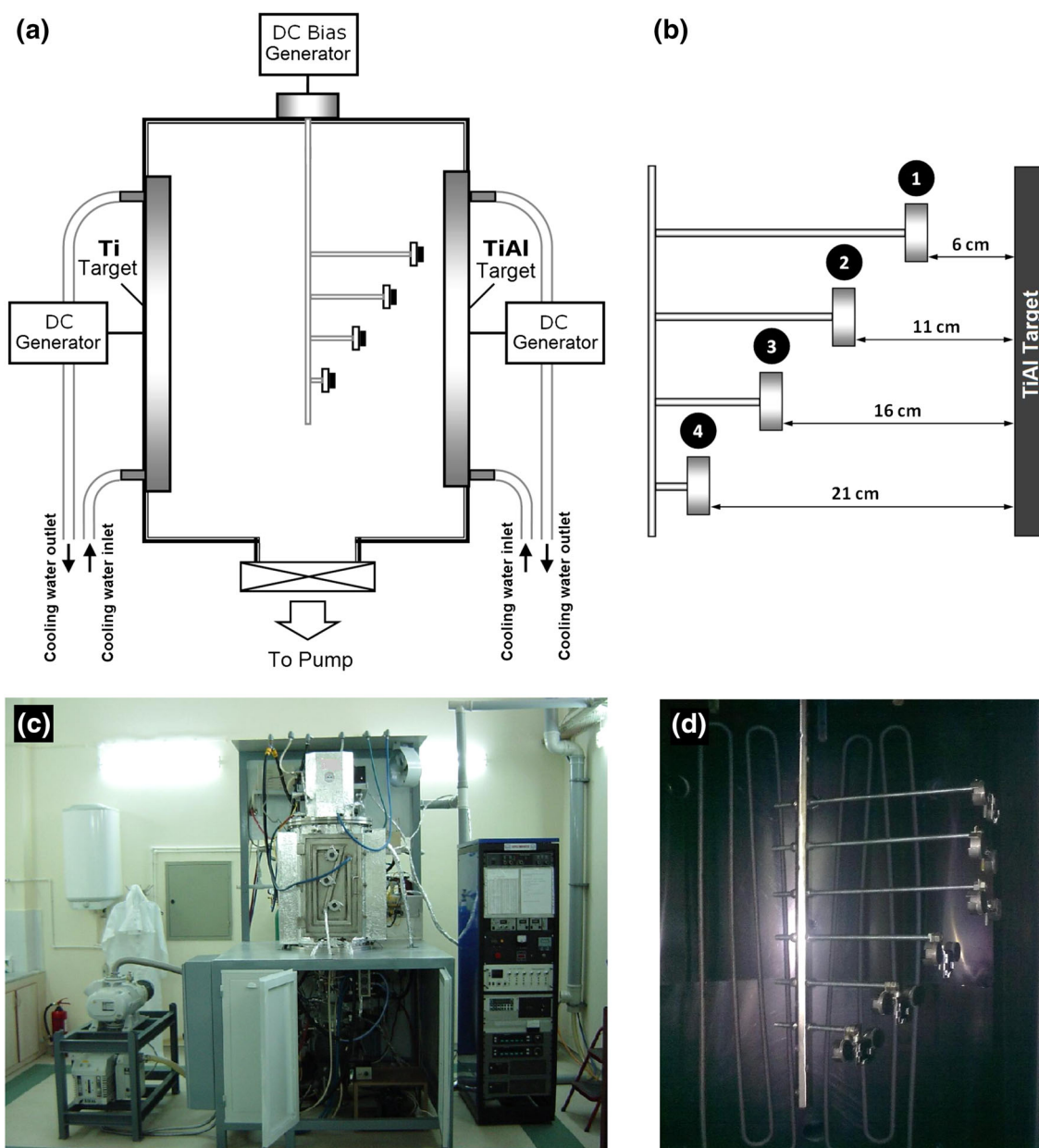


Fig. 1 Schematic illustrations of **a** magnetron sputtering coating system, **b** substrate holder and TSDs, pictures of **c** experimental set up, **d** substrate holder in vacuum chamber

ing parameters preliminary tests were conducted and nitrogen flow rate-cathode voltage-plasma emission (EMS) hysteresis behaviour was investigated. According to the results, the coating parameters were changed in the compound mode to ensure the growth of high-quality nitrides.

Prior to deposition, the substrates were ultrasonically cleaned in alcohol and also in acetone, each for 15 min, rinsed in distilled water, dried and then put into the deposition chamber. A stainless steel substrate holder was designed to set different TSDs, as seen in Fig. 1b. The pictures of experimental set up and substrate holder in vacuum chamber are shown in Fig. 1c, d. The TSDs were set 6, 11, 16 and 21

cm for each coating. The substrate holder was positioned in a static mode in front of the TiAl target and no turning was applied in the chamber. The substrate holder was also connected to an additional DC generator to apply ion bombardment for enhanced film adhesion. Argon and nitrogen were employed as the sputtering and the reactive gas, respectively. Mass flow rates were controlled with mass flow meters and pressures were measured with Baratron and Pirani pressure gauges. The deposition chamber was evacuated to a vacuum of about 3×10^{-2} mtorr and backfilled with argon gas to a pressure of 5 mtorr. First of all, the target was sputter cleaned in pure Ar to remove oxide and nitride layers on the target

surface with a desired DC power until a constant discharge voltage was reached. Then, the substrates were cleaned using Ar^+ ion bombardment for about 25 min at a negative DC substrate bias voltage of about 750 V. Prior to the growth of the TiAlN coating, a thin TiAl interlayer was deposited to enhance the adhesion of the coating to the substrate (30 s at 4,000 W target power). Then high purity nitrogen gas (99.998 %) was introduced to the system. The nitrogen flow control was used to obtain the desired target voltage for compound mode. Nitrogen pressures were changed between 0.3, 0.6 and 1.2 mtorr (4×10^{-2} , 8×10^{-2} and 1.6×10^{-1} Pa). TiAl target power was constant at 4,000 W and substrate bias voltages were changed between 0, -100 and -200 V. During the deposition process external heat was not used, and during the growth of the coating the temperature of the chamber was about 80°C , as measured by a thermocouple. The chamber walls were water-cooled during the deposition. The deposition time was 45 min for all coatings.

2.2 Characterization Techniques

All coatings were studied using scanning electron microscopy (LEO 440). The thickness of the coatings was measured using scanning electron microscopy and also by CSEM-Calotest. The deposition rates of the coatings were calculated from the overall thickness of the coatings divided by the total deposition time. The composition of the coatings was obtained using energy-dispersive X-ray spectroscopy. The atomic rates were calculated as the average of three measurements taken on different regions of each coating. The crystallographic structure and orientation of the coatings were studied using X-ray diffraction (Bruker AXS-D8 advanced) with $\text{Cu K}\alpha$ radiation. The main results of the mechanical properties, hardness (H) and elastic modulus (E), were recorded by CSEM nano-hardness tester using a Vickers indenter. The H and E values of the coatings were determined from the load-indentation curves using the Oliver-Pharr method [38], assuming a Poisson ratio of 0.30. Using a load of 15 mN the contribution from the substrate was regarded as very small or none for all coatings. The loading and unloading rates of the Vickers diamond indenter were 30 mN/min. In addition, the surfaces of the coatings were examined by atomic force microscopy (Veeco multimode nanoscope 3D) on a surface area of $2 \times 2 \mu\text{m}^2$ using tapping mode, and the Mahr profilometer. All the above-mentioned comparative properties were discussed.

3 Results and Discussion

3.1 Deposition Rates

The scanning electron micrographs of the fractured cross-sections of TiAlN coatings revealed that the coating thick-

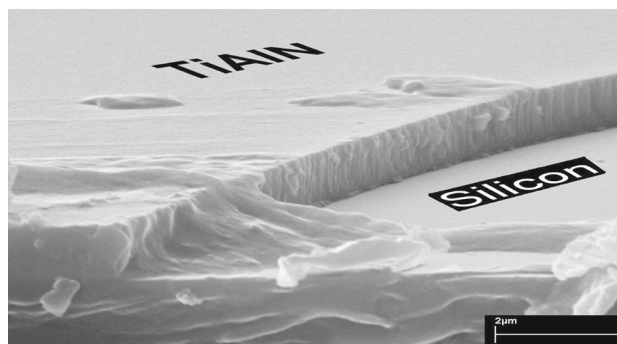


Fig. 2 The fractured cross-section of TiAlN coating deposited at nitrogen pressure of 1.2 mtorr, -100 V bias voltage and 16 cm TSD

nesses up to $5.2 \mu\text{m}$, and the deposition rates up to 115.5 nm/min were achieved. In addition, the thickness of the TiAl interlayers was found as 303, 170, 125 and 105 nm for 6, 11, 16 and 21 cm TSDs, respectively. The scanning electron microscope image of the fractured cross-section of TiAlN coating deposited at nitrogen pressure of 1.2 mtorr, -100 V bias voltage and 16 cm TSD can be seen in Fig. 2. There it was seen that all the coatings deposited by different coating parameters generally exhibit a columnar structure with a relatively compact structure and pore-free surfaces. The variations of deposition rate of the coatings with TSD for different nitrogen pressures and bias voltages are given in Fig. 3. The results showed that increasing the TSD and nitrogen pressure caused a decrease in the deposition rate for all coatings. At high nitrogen pressures, the poisoning of the magnetron targets and the collision and scattering of the atoms and molecules become significant, and reduce the number and kinetic energy of the species approaching the substrate. The deposition rate of the coatings can be significantly reduced at high nitrogen pressures but some models including TSD, magnetron power and bias voltage must be used to develop overall understanding [29]. A decrease in deposition rate with increasing total ($\text{Ar} + \text{N}_2$) pressure can be attributed to increased scattering losses as decreasing of the mean free path (MFP) [34]. It was also found that a significantly large increase in deposition rates was observed at 6 cm TSD. Between the 11 and 21 cm TSDs the deposition rates were relatively constant. No significant change was observed with bias voltage.

3.2 Coating Compositions

The variation of atomic Al/Ti ratios and the nitrogen contents of the coatings with TSD for different nitrogen pressures and bias voltages are shown in Figs. 4 and 5, respectively. Chen et al. [34] concluded that losses due mainly to the scattering and angular distribution of the sputter flux, together with the different poisoning state of the Ti and Al particles of the

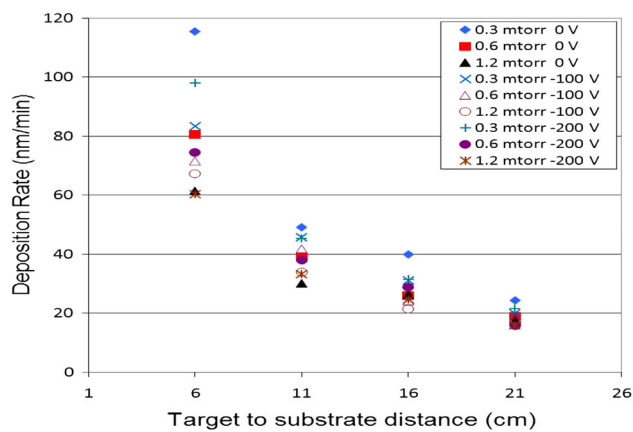


Fig. 3 Variation of deposition rate of the coatings with TSD for different nitrogen pressures and bias voltages

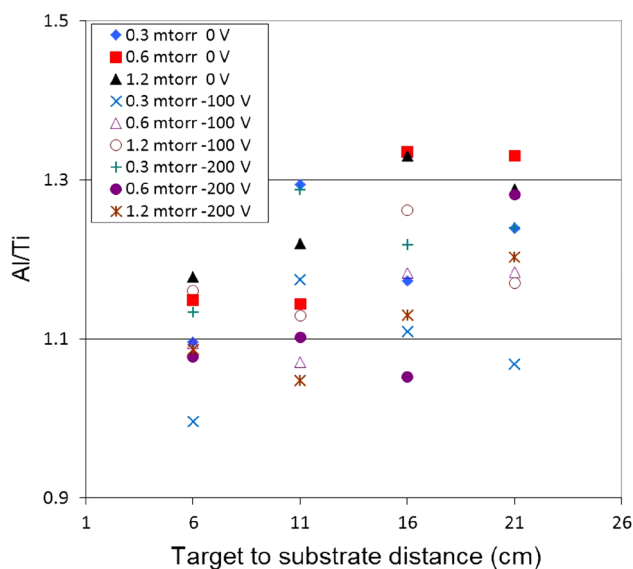


Fig. 4 Variation of Al/Ti ratio of the coatings with TSD for different nitrogen pressures and bias voltages

powder-metallurgically prepared $Ti_{0.5}Al_{0.5}$ target, led to a huge deviation in the Al/Ti ratio of the films as compared to the target, which is clearly identified with the present results. Except for 0.996, all the films investigated maintained higher Al/Ti ratios than the target for all deposition parameters used in this study, as seen in Fig. 4.

Increasing the TSD generally resulted in increased Al/Ti ratios too. At 0.3 mtorr nitrogen pressure, a remarkable increase in Al/Ti ratio is found when TSD increases from 6 to 11 cm. At the same nitrogen pressure, the Al/Ti ratio decreases again at 16 cm TSD. The increase at 0.3 mtorr nitrogen pressure and 11 cm TSD is not observed at 0.6 and 1.2 mtorr nitrogen pressures. The maximum Al/Ti ratio of 1.34 is found at 0 V bias voltage, 0.6 mtorr nitrogen pressure and 16 cm TSD. At 0.3 mtorr nitrogen pressure, Al/Ti ratios

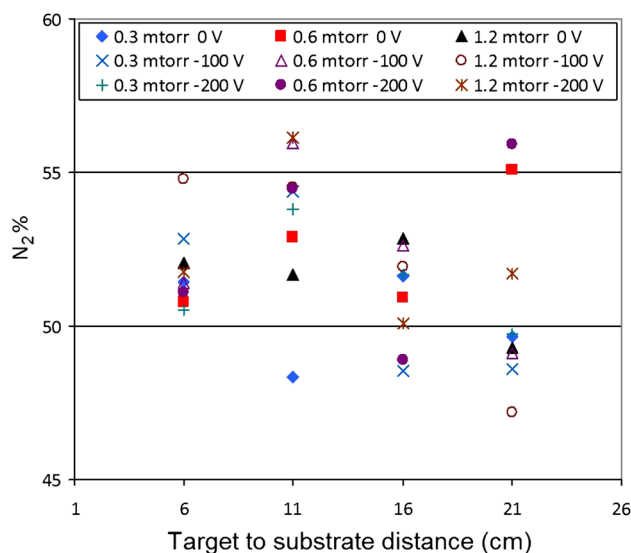


Fig. 5 Variation of nitrogen content of the coatings with TSD for different nitrogen pressures and bias voltages

decrease with increasing bias voltage from 0 to -100 V and increase again with increasing bias voltage from -100 to -200 V. This increase in Al/Ti ratio at -200 V bias voltage is not observed at 0.6 and 1.2 mtorr nitrogen pressures. The 21 cm TSD is found as a critical distance, because the Al/Ti ratio increases again with increasing bias voltage from -100 to -200 V at 21 cm TSD. The back scattering of target atoms from the substrate increases at higher bias voltages. In addition, Al atoms can back scatter much more as compared with heavier Ti atoms. Consequently, increasing the bias voltage generally resulted in decreased Al/Ti ratios. Furthermore, the 11 cm TSD is also found as an important distance for 0.3 mtorr nitrogen pressure. Ti particles of the powder metallurgically prepared $Ti_{0.5}Al_{0.5}$ target are more easily poisoned than the Al particles. Consequently, when the Ti particles are already poisoned, the Al particles can still be in metallic mode and different compositions can be found at different deposition conditions [34].

Although the detection efficiency of low atomic mass number elements such as nitrogen is low in energy-dispersive X-ray spectroscopy analysis the relative nitrogen contents (at.%) of the coatings deposited at different parameters were also investigated (Fig. 5). Elemental analysis showed that the nitrogen contents of the coatings up to 56 % were achieved and were not influenced significantly by the deposition parameters because of the compound mode used in this study. At conditions of 11 cm TSD, 1.2 mtorr nitrogen pressure and -200 V bias voltage, the nitrogen content is found to be higher than the others. Furthermore, in regard to nitrogen contents, a small increase is found when nitrogen pressure is increased, also a decrease is found when TSD is increased, as can be seen in Fig. 5. This was attributed to the position

of the nitrogen gas inlet in the chamber. Nitrogen gas was sent into the chamber near the target surface and expanded towards the interior. With bias voltage, no significant change was observed in the nitrogen contents of the films. However, nitrogen content tends to increase with increasing bias voltage from 0 to -100 V and decreases again with increasing bias voltage from -100 to -200 V, at 6 and 11 cm TSDs. In contrast, nitrogen content decreases with increasing bias voltage from 0 to -100 V and increases with increasing bias voltage from -100 to -200 V, at 21 cm TSD. Consequently, the 11 cm TSD is found as an important parameter for the nitrogen content of the coatings.

3.3 Crystal Structures

X-ray diffraction patterns recorded from TiAlN films deposited on Si(100) substrates showed that TiAlN present the cubic B1 structure with major preferential orientations along the (1 1 1) and (2 0 0). The X-ray diffraction patterns of films deposited at 0 V bias voltage, 6 cm TSD and 0.3–1.2 mtorr nitrogen pressures are shown in Fig. 6. It was found that when nitrogen pressure was increased from 0.3 to 1.2 mtorr, the intensity of (1 1 1) sharply increased, and the grain size also increased from 36 to 45 nm, at 6 cm TSD. X-ray diffraction patterns of the films deposited at -200 V bias voltage, 16 cm TSD and 0.3–1.2 mtorr nitrogen pressures are also given in Fig. 6. With increasing nitrogen pressure, the peak reflections were found to decrease. Furthermore, a strong development of (2 0 0) component was found at -200 V bias voltage and 0.3 mtorr nitrogen pressure, which was not seen at 0 V bias voltage. Bias voltage applied to the substrate has a significant effect on ion-energies. When increasing ion-energies the peak reflection of (1 1 1) is able to change to (2 0 0) preferential orientation in TiAlN films [39]. Deposition at high bias voltages is resulted in a coating structure containing large single crystalline domains [40]. In addition, the use of higher bias voltages is resulted densification of grain boundaries with a corresponding decrease in average grain size [41]. Increasing the nitrogen pressure also caused a small decrease in grain size from 8 to 6 nm, at 16 cm TSD. With increasing the TSD, the peak reflection of (1 1 1) increased when the peak reflection of (2 0 0) decreased at -100 V bias voltage and 0.6 mtorr nitrogen pressure, as can be seen in Fig. 7. The grain sizes were found 14.5, 18.5, 34.5 and 39.5 nm at 6, 11, 16 and 21 cm TSD, respectively. Consequently, X-ray diffraction analysis in this study showed that short TSDs and high bias voltages indicated significant effect on a (2 0 0) oriented structure.

3.4 Mechanical Properties

Nano-hardness measurements revealed that the hardness of the coatings up to 2,916 HV and that the elastic modulus up

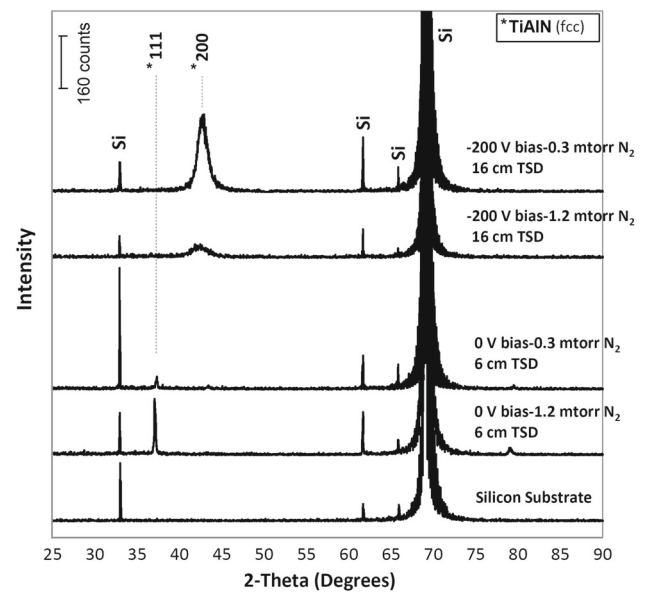


Fig. 6 X-ray diffraction patterns of TiAlN coatings grown for 0 V bias voltage, 6 cm TSD and -200 V bias voltage, 16 cm TSD at 0.3 and 1.2 mtorr nitrogen pressures

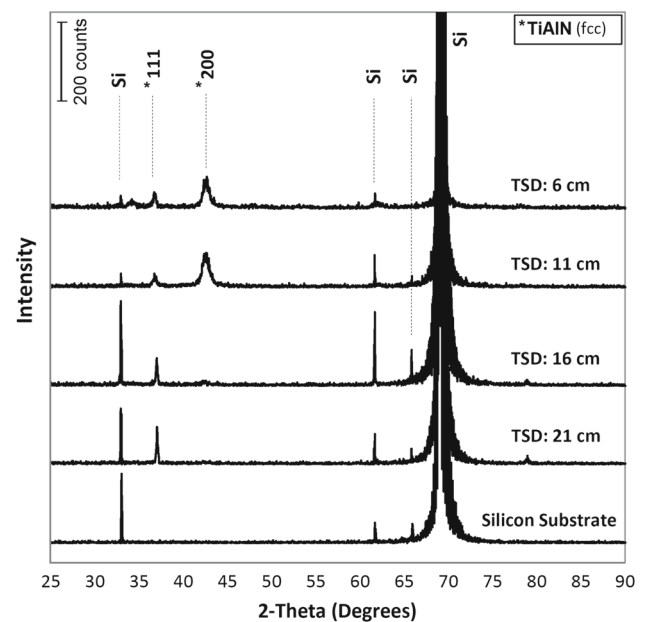


Fig. 7 X-ray diffraction patterns of TiAlN coatings grown for -100 V bias voltage and 0.6 mtorr nitrogen pressure at different TSDs

to 340 GPa were achieved. Indentation depths up to 195 nm were achieved under the load of 15 mN. The variation of the hardness and the elastic modulus of the coatings with TSD for different coating parameters are given in Figs. 8 and 9, respectively.

The results showed that increasing the TSD caused a decrease in both the hardness and the elastic modulus of the coatings. The kinetic energy of depositing atoms/molecules

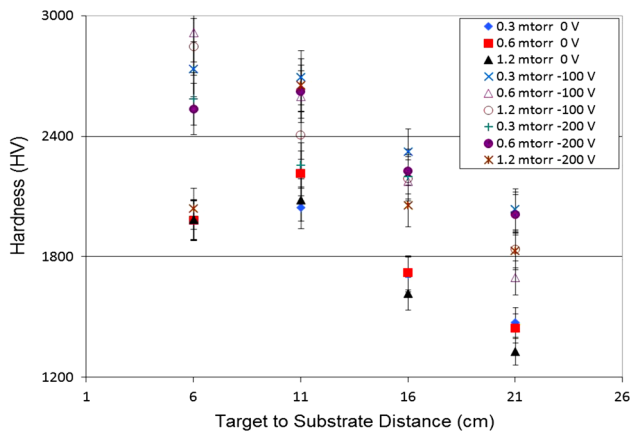


Fig. 8 Variation of hardness of the coatings with TSD for different nitrogen pressures and bias voltages

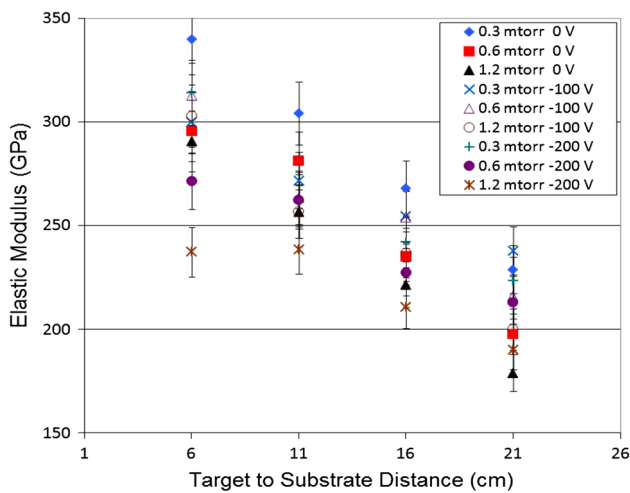


Fig. 9 Variation of elastic modulus of the coatings with TSD for different nitrogen pressures and bias voltages

has been considered as a major factor affecting the adatom mobility and formation of the nucleated clusters. With higher depositing energies, the nucleation rate will be enhanced and coatings with smaller grain sizes develop [29]. The energies of depositing species are higher for short TSDs and cause a dense microstructure with high hardness. Lower nitrogen pressures have a similar effect on the kinetic energy of the species approaching the substrate, as mentioned before. Increasing the nitrogen pressure results in decreasing the elastic modulus of the coatings (Fig. 9). In the case of hardness, this decrease was found at 16 and 21 cm TSDs, as seen in Fig. 8. Furthermore, the 11 cm TSD was found as the critical distance for enhanced hardness at 0 V bias voltage and all nitrogen pressures. The hardness of the coatings were found to give similar peak values at -200 V bias voltage, 11 cm TSD, 0.6 and 1.2 mtorr nitrogen pressures. Increasing the bias voltage generally results in increasing hardness. However, -100 V bias voltage was found to give maximum

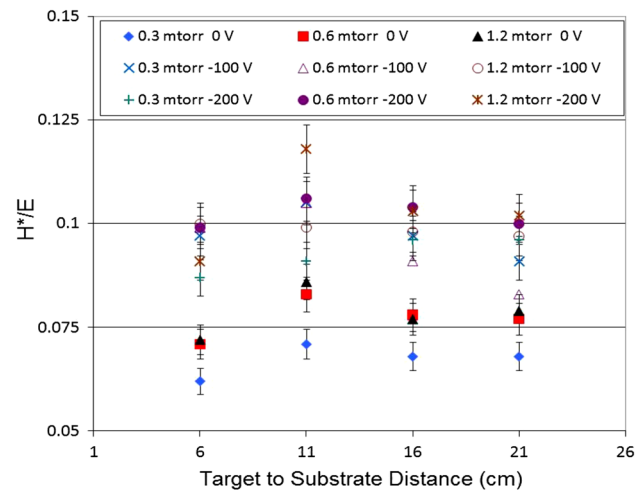


Fig. 10 Variation of H/E ratio of the coatings with TSD for different nitrogen pressures and bias voltages (*in GPa)

hardness for 6 cm TSD. In the case of elastic modulus, the increase at -100 V bias voltage was found at 0.6 and 1.2 mtorr nitrogen pressures.

The H/E ratio, which is proportional to the resistance of the film to plastic deformation, was determined for all coatings, as can be seen in Fig. 10. 0 V bias voltage was found to give minimum H/E ratios for the films, similar to the hardness values. The H/E ratio is also widely quoted as a valuable measure in determining the limit of elastic behaviour in a surface contact, which is clearly important for the avoidance of wear [42]. Furthermore, the H/E ratios of the coatings were found to be higher at 0.6 and 1.2 mtorr nitrogen pressures than at 0.3 mtorr. No significant change was observed with TSD. However, the 11 cm TSD was also found to give a peak value for the H/E ratios.

3.5 Surface Properties

The variation of surface roughness of the coatings with TSD for different parameters is shown in Fig. 11. The R_a values of the coatings were calculated as the average of four measurements taken on different regions of each coating. The results showed that R_a values of the coatings up to 6 nm were achieved with respect to deposition parameters. In the literature, it is reported that the surface texture becomes smoother with increased bias voltage and decreased nitrogen pressure and also TSD [4,29]. From Fig. 11, although no specific change was observed with coating parameters in R_a values, a slight decrease was found when TSD increased from 6 to 21 cm. However, at 0.6 mtorr nitrogen pressure, 0 and -100 V bias voltages, surface roughness values tend to increase after the 11 cm TSD. Furthermore, a similar increase in R_a values after 11 cm TSD is also seen at -200 V bias voltage. -100 V bias voltage is found to give higher R_a values than

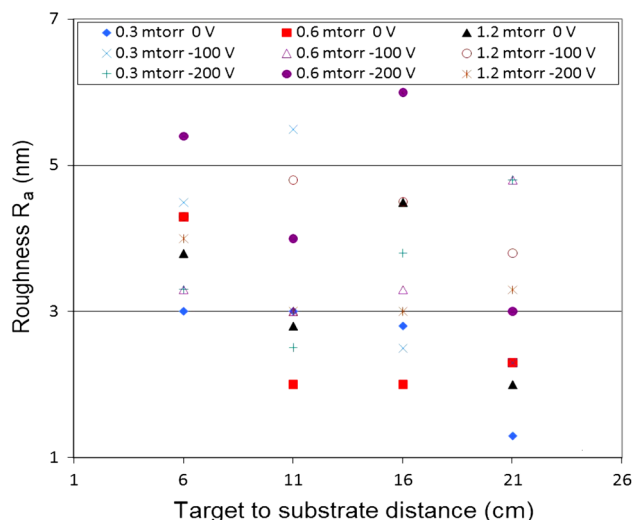
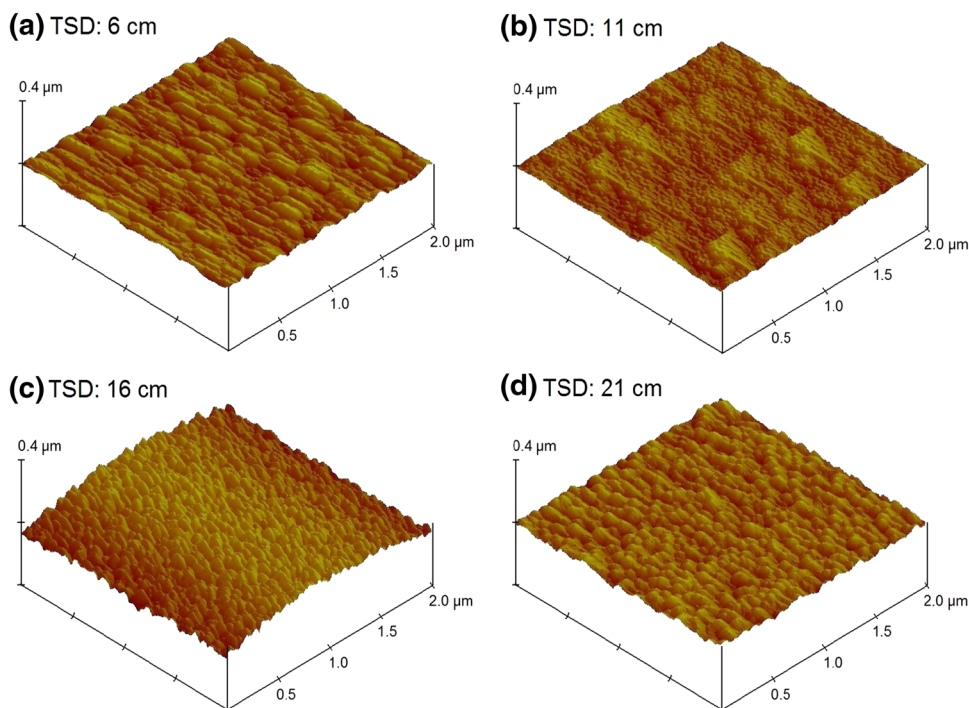


Fig. 11 Variation of surface roughness of the coatings with TSD for different nitrogen pressures and bias voltages

–200 V at 0.3 mtorr nitrogen pressure, 6–11 cm TSDs, and also at 1.2 mtorr nitrogen pressure.

The surface properties of the coatings were also investigated by atomic force microscopy. The atomic force microscope images of the coatings grown for –100 V bias voltage, 0.6 mtorr nitrogen pressure and different TSDs are shown in Fig. 12. The results show that all the coatings exhibit a columnar structure and the columns are homogeneously distributed vertical to the deposition direction as demonstrated by scanning electron microscopy. Each column has a dome on the coating surface in nanometric scale height. The atomic

Fig. 12 Atomic force microscope images of TiAlN coatings grown for –100 V bias voltage, 0.6 mtorr nitrogen pressure and **a**, **b** 11, **c** 16 and **d** 21 cm TSDs



force microscope images also indicate that the coatings have pore-free surfaces with no micro-cracks. The 11 cm TSD is found to give the smoothest surface morphology (R_a 3.0 nm) at –100 V bias voltage and 0.6 mtorr nitrogen pressure, as seen in Fig. 12b. The coatings deposited at 0 V bias voltage are found to have relatively large columns. The dense microstructure of the coatings deposited at –100 and –200 V bias voltages is attributed to ion bombardment during deposition. Bias voltage resulted in coatings with a fine-grained morphology. This is also demonstrated by hardness enhancement at high bias voltages. The optical microscope (Nikon) images and the pictures of the coatings grown for –100 V bias voltage, 0.6 mtorr nitrogen pressure and different TSDs are shown in Fig. 13.

4 Conclusions

From the above study on TiAlN films deposited on Si(100) substrates by DC magnetron sputtering, the following conclusions can be drawn:

TSD showed a significant effect on the microstructure and mechanical properties of the coatings. Decreasing the TSD and nitrogen pressure caused an increase in the deposition rate for all coatings as a result of decreased scattering losses. A maximum deposition rate of 115.5 nm/min was achieved at 0 V bias voltage, 0.3 mtorr nitrogen pressure and 6 cm TSD.

Increasing the bias voltage generally resulted in decreasing Al/Ti ratios because of the back scattering of lighter Al

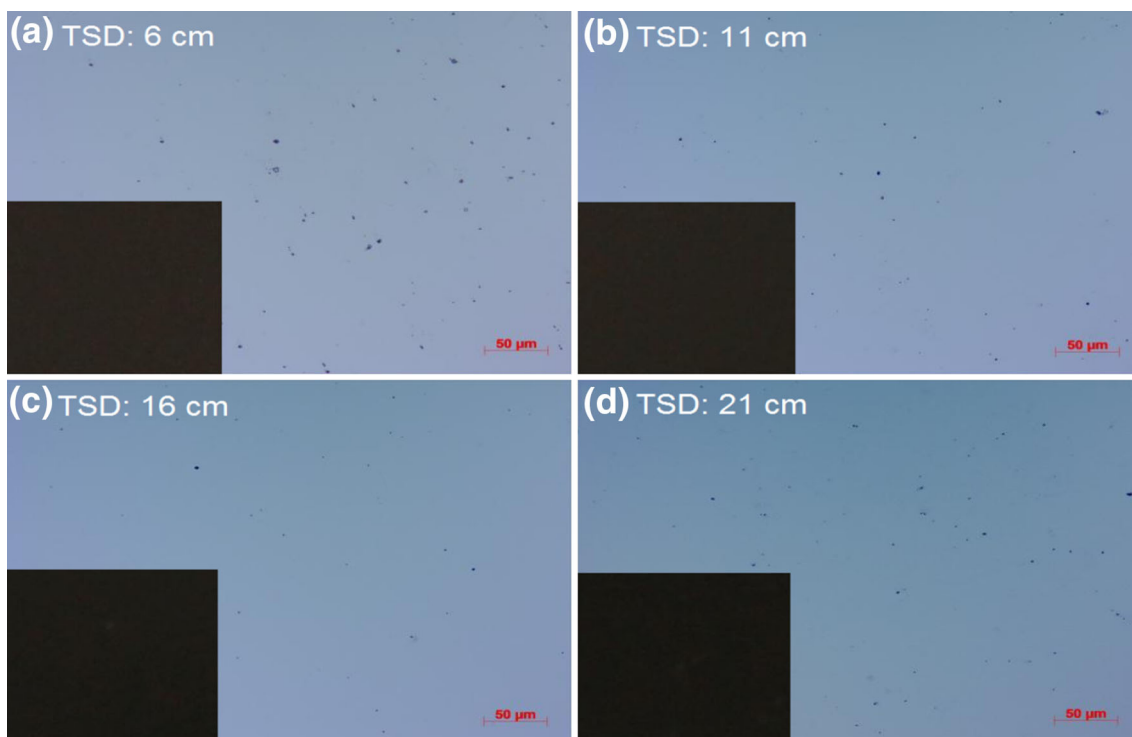


Fig. 13 Optical microscope images and pictures of TiAlN coatings grown for -100 V bias voltage, 0.6 mtorr nitrogen pressure and **a** 6 , **b** 11 , **c** 16 and **d** 21 cm TSDs

atoms from the substrate. Furthermore, decreasing the TSD also resulted in decreasing Al/Ti ratios. The 11 cm TSD was found to be an important distance for enhanced Al/Ti ratio at 0.3 mtorr nitrogen pressure. In regard to nitrogen contents, a small increase is found when nitrogen pressure is increased, also a decrease is found when TSD is increased.

From the indentation tests it was found that decreasing the TSD caused an increase in both the hardness and the elastic modulus of the coatings because of the high kinetic energies of the species approaching the substrate. High bias voltage and low nitrogen pressure were found to have a similar effect on hardness. The paper also revealed a correlation between grain size and coating hardness. For decreased crystallite size, hardness increased especially at short TSDs and high bias voltages which resulted a $(2\ 0\ 0)$ -oriented structure. The fine-grained morphology of the coatings with increased bias voltage was also demonstrated by atomic force microscopy. Furthermore, the 11 cm TSD showed a critical behaviour for enhanced hardness at 0 V bias voltage. However, 0 V bias voltage was found to give minimum H/E ratios for the films, similar to hardness values, as compared to -100 and -200 V bias voltages.

Acknowledgments This work was held in the Surface Technologies Research and Application Laboratory and was supported by the Office of Scientific Research Projects in Erciyes University (Project No: FBT-07-50).

References

- Urtekin, L.; Kucukturk, G.; Karacay, T.; Uslan, I.; Salman, S.: An investigation of thermal properties of zirconia coating on aluminum. *Arabian J. Sci. Eng.* **37**(8), 2323–2332 (2012)
- Witkea, U.; Schuelkeb, T.; Schultricha, B.; Siemrotha, P.; Vetter, J.: Comparison of filtered high-current pulsed arc deposition f-HCA with conventional vacuum arc methods. *Surf. Coat. Technol.* **126**, 81–88 (2000)
- Kelly, P.J.; Arnell, R.D.: Magnetron sputtering: a review of recent developments and applications. *Vacuum* **56**, 159–172 (2000)
- PalDey, S.; Deevi, S.C.: Single layer and multilayer wear resistant coatings of (Ti, Al)N: a review. *Mater. Sci. Eng. A* **342**, 58–79 (2003)
- Ersen, O.; Tuilier, M.-H.; Thobor-Keck, A.; Rousselot, C.; Cortès, R.: Relation between interfacial structure and mechanical properties in AlN/TiN bilayers investigated by EXAFS. *Nucl. Instr. Meth. B* **234**, 308–320 (2005)
- Suresha, S.J.; Bhide, R.; Jayaram, V.; Biswas, S.K.: Processing, microstructure and hardness of TiN/(Ti, Al)N multilayer coatings. *Mater. Sci. Eng. A* **429**, 252–260 (2006)
- William Grips, V.K.; Barshilia, H.C.; Ezhil Selvi, V.; Kalavati Rajam, K.S.: Electrochemical behavior of single layer CrN, TiN, TiAlN coatings and nanolayered TiAlN/CrN multilayer coatings prepared by reactive direct current magnetron sputtering. *Thin Solid Films* **514**, 204–211 (2006)
- Xiang, Y.; Hua, M.; Cheng-biao, W.; Zhi-qiang, F.; Yang, L.: Investigation of Ti/TiN multilayered films in a reactive mid-frequency dual-magnetron sputtering. *Appl. Surf. Sci.* **253**, 3705–3711 (2007)
- Quesada, F.; Mariño, A.; Restrepo, E.: TiAlN coatings deposited by r.f. magnetron sputtering on previously treated ASTM A36 steel. *Surf. Coat. Technol.* **201**, 2925–2929 (2006)

10. Fukumoto, N.; Ezura, H.; Yamamoto, K.; Hotta, A.; Suzuki, T.: Effects of bilayer thickness and post-deposition annealing on the mechanical and structural properties of (Ti,Cr,Al)N/(Al,Si)N multilayer coatings. *Surf. Coat. Technol.* **203**, 1343–1348 (2009)
11. Hsieh, J.H.; Liang, C.; Yu, C.H.; Wu, W.: Deposition and characterization of TiAlN and multi-layered TiN/TiAlN coatings using unbalanced magnetron sputtering. *Surf. Coat. Technol.* **108–109**, 132–137 (1998)
12. Raveh, A.; Weiss, M.; Pinkas, M.; Rosen, D.Z.; Kimmel, G.: Graded Al–AlN, TiN, and TiAlN multilayers deposited by radio-frequency reactive magnetron sputtering. *Surf. Coat. Technol.* **114**, 269–277 (1999)
13. Khrais, S.K.; Lin, Y.J.: Wear mechanisms and tool performance of TiAlN PVD coated inserts during machining of AISI 4140 steel. *Wear* **262**, 64–69 (2007)
14. Santana, A.E.; Karimi, A.; Derflinger, V.H.; Schütze, A.: Microstructure and mechanical behavior of TiAlCrN multilayer thin films. *Surf. Coat. Technol.* **177–178**, 334–340 (2004)
15. Wadsworth, I.; Smith, I.J.; Donohue, L.A.; Münz, W.-D.: Thermal stability and oxidation resistance of TiAlN/CrN multilayer coatings. *Surf. Coat. Technol.* **94–95**, 315–321 (1997)
16. Salas, O.; Kearns, K.; Carrera, S.; Moore, J.J.: Tribological behavior of candidate coatings for Al die casting dies. *Surf. Coat. Technol.* **172**, 117–127 (2003)
17. Panjan, P.; Bončina, I.; Bevk, J.; Čekada, M.: PVD hard coatings applied for the wear protection of drawing dies. *Surf. Coat. Technol.* **200**, 133–136 (2005)
18. Thobor, A.; Rousselot, C.; Clement, C.; Takadoum, J.; Martin, N.; Sanjines, R.; Levy, F.: Enhancement of mechanical properties of TiN/AlN multilayers by modifying the number and the quality of interfaces. *Surf. Coat. Technol.* **124**, 210–221 (2000)
19. Hovsepian, P.Eh.; Lewis, D.B.; Luo, Q.; Münz, W.-D.; Mayrhofer, P.H.; Mitterer, C.; Zhou, Z.; Rainforth, W.M.: TiAlN based nanoscale multilayer coatings designed to adapt their tribological properties at elevated temperatures. *Thin Solid Films* **485**, 160–168 (2005)
20. Manaila, R.; Devenyi, A.; Biro, D.; David, L.; Barna, P.B.; Kovacs, A.: Multilayer TiAlN coatings with composition gradient. *Surf. Coat. Technol.* **151–152**, 21–25 (2002)
21. Tönshoff, K.; Karpuschewski, B.; Mohlfeld, A.; Leyendecker, T.; Erkens, G.; Fuß, H.G.; Wenke, R.: Performance of oxygen-rich TiAlON coatings in dry cutting applications. *Surf. Coat. Technol.* **108–109**, 535–542 (1998)
22. Derflinger, V.H.; Schütze, A.; Ante, M.: Mechanical and structural properties of various alloyed TiAlN-based hard coatings. *Surf. Coat. Technol.* **200**, 4693–4700 (2006)
23. Tentardini, E.K.; Aguzzoli, C.; Castro, M.; Kunrath, A.O.; Moore, J.J.; Kwietniewski, C.; Baumvol, I.J.R.: Reactivity between aluminum and (Ti,Al)N coatings for casting dies. *Thin Solid Films* **516**, 3062–3069 (2008)
24. Neidhardt, J.; Mráz, S.; Schneider, J.M.; Strub, E.; Bohne, W.; Liedke, B.; Möller, W.; Mitterer, C.: Experiment and simulation of the compositional evolution of Ti–B thin films by sputtering of a compound target. *J. Appl. Phys.* **104**, 063304 (2008)
25. Jeong, J.J.; Hwang, S.K.; Lee, C.M.: Nitrogen flow rate dependence of the growth morphology of TiAlN films deposited by reactive sputtering. *Surf. Coat. Technol.* **151–152**, 82–85 (2002)
26. Ramana, J.V.; Kumar, S.; David, C.; Raju, V.S.: Structure, composition and microhardness of (Ti, Zr)N and (Ti, Al)N coatings prepared by dc magnetron sputtering. *Mater. Lett.* **58**, 2553–2558 (2004)
27. Oliveira, J.C.; Manaia, A.; Cavaleiro, A.; Vieira, M.T.: Structure, hardness and thermal stability of Ti(Al,N) coatings. *Surf. Coat. Technol.* **201**, 4073–4077 (2006)
28. Oliveira, J.C.; Manaia, A.; Dias, J.P.; Cavaleiro, A.; Teer, D.; Taylor, S.: The structure and hardness of magnetron sputtered Ti–Al–N thin films with low N contents (<42 at.%). *Surf. Coat. Technol.* **200**, 6583–6587 (2006)
29. Wuhrer, R.; Yeung, W.Y.: Effect of target-substrate working distance on magnetron sputter deposition of nanostructured titanium aluminium nitride coatings. *Scripta Mater.* **49**, 199–205 (2003)
30. Barshilia, H.C.; Yogesh, K.; Rajam, K.S.: Deposition of TiAlN coatings using reactive bipolar-pulsed direct current unbalanced magnetron sputtering. *Vacuum* **83**, 427–434 (2009)
31. Ahlgren, M.; Blomqvist, H.: Influence of bias variation on residual stress and texture in TiAlN PVD coatings. *Surf. Coat. Technol.* **200**, 157–160 (2005)
32. Zywitzki, O.; Klostermann, H.; Fietzke, F.; Modes, T.: Structure of superhard nanocrystalline (Ti, Al)N layers deposited by reactive pulsed magnetron sputtering. *Surf. Coat. Technol.* **200**, 6522–6526 (2006)
33. You, Y.Z.; Kim, D.: Influence of incidence angle and distance on the structure of aluminium nitride films prepared by reactive magnetron sputtering. *Thin Solid Films* **515**, 2860–2863 (2007)
34. Chen, L.; Moser, M.; Du, Y.; Mayrhofer, P.H.: Compositional and structural evolution of sputtered Ti–Al–N. *Thin Solid Films* **517**, 6635–6641 (2009)
35. Panich, N.; Sun, Y.: Effect of substrate rotation on structure, hardness and adhesion of magnetron sputtered TiB₂ coating on high speed steel. *Thin Solid Films* **500**, 190–196 (2006)
36. Danisman, K.; Danisman, S.; Savas, S.; Dalkiran, I.: Modelling of the hysteresis effect of target voltage in reactive magnetron sputtering process by using neural networks. *Surf. Coat. Technol.* **204(5)**, 610–614 (2009)
37. Rossnagel, S.M.: Thin film deposition with physical vapour deposition and related technologies. *J. Vac. Sci. Technol. A* **21(5)**, 74–87 (2003)
38. Oliver, W.C.; Pharr, G.M.: An improved technique for determining hardness and elastic modulus using load and displacement sensing indentation experiments. *J. Mater. Res.* **76**, 1564–1583 (1992)
39. Pfeiler, M.; Kutschej, K.; Penoy, M.; Michotte, C.; Mitterer, C.; Kathrein, M.: The influence of bias voltage on structure and mechanical/tribological properties of arc evaporated Ti–Al–V–N coatings. *Surf. Coat. Technol.* **202**, 1050–1054 (2007)
40. Sáfrán, G.; Reinhard, C.; Ehasarian, A.P.; Barna, P.B.; Székely, L.; Geszti, O.; Hovsepian, P.Eh.: Influence of the bias voltage on the structure and mechanical performance of nanoscale multilayer CrAlYN/CrN physical vapor deposition coatings. *J. Vac. Sci. Technol. A* **27(2)**, 174–182 (2009)
41. Petrov, I.; Hultman, L.; Sundgren, J.-E.; Greene, J.E.: Polycrystalline TiN films deposited by reactive bias magnetron sputtering: effects of ion bombardment on resputtering rates, film composition, and microstructure. *J. Vac. Sci. Technol. A* **10(2)**, 265–272 (1992)
42. Leyland, A.; Matthews, A.: On the significance of the H/E ratio in wear control: a nanocomposite coating approach to optimised tribological behaviour. *Wear* **246**, 1–11 (2000)